

Discovery of benzamide analogs as negative allosteric modulators of human neuronal nicotinic receptors: Pharmacophore modeling and structure–activity relationship studies

Bitna Yi^{a,†}, Sihui Long^{b,†}, Tatiana F. González-Cestari^a, Brandon J. Henderson^{a,‡}, Ryan E. Pavlovicz^c, Karl Werbovetz^b, Chenglong Li^{b,c}, Dennis B. McKay^{a,*}

^a Division of Pharmacology, College of Pharmacy, The Ohio State University, 500 West 12th Avenue, Columbus, OH 43210, USA

^b Division of Medicinal Chemistry and Pharmacognosy, College of Pharmacy, The Ohio State University, Columbus, OH 43210, USA

^c Biophysics Program, The Ohio State University, Columbus, OH 43210, USA

ARTICLE INFO

Article history:

Received 9 January 2013

Revised 22 March 2013

Accepted 29 March 2013

Available online 6 April 2013

Keywords:

Neuronal nicotinic receptors
Negative allosteric modulators
Structure–activity relationship studies
Pharmacophore modeling

ABSTRACT

The present study describes our ongoing efforts toward the discovery of drugs that selectively target nAChR subtypes. We exploited knowledge on nAChR ligands and their binding site that were previously identified by our laboratory through virtual screenings and identified benzamide analogs as a novel chemical class of neuronal nicotinic receptor (nAChR) ligands. The lead molecule, compound **1** (4-(allyloxy)-N-(6-methylpyridin-2-yl)benzamide) inhibits nAChR activity with an IC₅₀ value of 6.0 (3.4–10.6) μM on human α4β2 nAChRs with a ~5-fold preference against human α3β4 nAChRs. Twenty-six analogs of compound **1** were also either synthesized or purchased for structure–activity relationship (SAR) studies and provided information relating the chemical/structural properties of the molecules to their ability to inhibit nAChR activity. The discovery of subtype-selective ligands of nAChRs described here should contribute significantly to our understanding of the involvement of specific nAChR subtypes in normal and pathophysiological states.

© 2013 Published by Elsevier Ltd.

1. Introduction

Neuronal nicotinic acetylcholine receptors (nAChRs) are ligand-gated ion channels that mediate the physiological effects elicited by the endogenous neurotransmitter, acetylcholine (ACh). nAChR signaling influences and regulates a number of physiologically important processes (e.g., cognition, arousal, anxiety, pain processing, food intake, and reward).^{1,2} Furthermore, disruption or alteration of nAChR activity has been implicated in many diseases and disorders (Alzheimer's disease, Parkinson's disease, depression, schizophrenia, and addiction).³ Therefore, nAChRs hold considerable promise as therapeutic targets.

A major challenge in the study of the nAChRs is the diversity and complexity of these pentameric receptors. There are eleven

Abbreviations: NAM, negative allosteric modulator; nAChRs, neuronal nicotinic acetylcholine receptors; HBK, HEPES-buffered Krebs; LBVS, ligand-based virtual screening; SBVS, structure-based virtual screening; SAR, structure–activity relationship; n_H , Hill coefficient.

* Corresponding author. Address: Division of Pharmacology, The Ohio State University, College of Pharmacy, 500 West 12th Avenue, Columbus, Ohio 43210, USA. Tel.: +1 614 292 3771; fax: +1 614 292 9083.

E-mail address: Mckay.2@osu.edu (D.B. McKay).

† These authors contributed equally to the work.

‡ Present address: Division of Biology, California Institute of Technology, Pasadena, CA 91125, USA.

human genes that encode nAChR subunits (α2–α10 excluding α8 and β2–β4). These subunits assemble to form multiple subtypes that are characterized by distinct biochemical properties (e.g., ion selectivity, conductance, mean channel open time, permeability to Ca²⁺, and desensitization rate).^{4–6} Importantly, each subunit is expressed in unique spatial and developmental patterns, suggesting the possibility that individual subtypes may play distinct roles in certain physiological processes.^{6,7} Knowledge of these roles will pave the way toward the identification of novel therapeutic targets and allow the development of more targeted pharmacotherapy with reduced side effects. Therefore, drugs that specifically target nAChR subtypes can represent valuable research tools by providing insight into the roles that different nAChR subtypes play in physiological and pathological states.

Orthosteric binding sites of nAChRs (sites of ACh binding) contain a high level of sequence homology. At the interface between α and β subunits, ACh interacts with the 'aromatic nest', which is a group of five aromatic amino acid residues (i.e., Trp56, Trp61, Trp87, Trp150, and Tyr199). (The numbers used in this manuscript are based on the first transcribed protein). These residues are completely conserved in all nAChR subunits.¹⁸ In addition, amino acid residues surrounding the orthosteric site (Cys 193, Cys 194, and Tyr 94) are also completely conserved or highly conserved (75–100% amino acid identity across nAChR subunits). We believe

that this extensive level of sequence homology makes it difficult to discover and develop drugs that interact with the orthosteric binding site and pharmacologically discriminate one subtype from others. Our laboratory is addressing the issue of subtype-selectivity by targeting ‘non-orthosteric’ sites of nAChRs previously identified by our laboratory (e.g., allosteric sites).¹⁶ Our hypotheses are that (1) structural variations within allosteric binding sites can provide a foundation to develop subtype-selective ligands of nAChRs and (2) a multidisciplinary approach can direct the design and synthesis of new molecules with optimized properties (i.e., selectivity and potency). The present study is a proof-of-concept study to document the utilization of allosteric binding sites to develop drugs with specificity for nAChR subtypes using a combination of multiple approaches. In particular, we focused on the subtype-selectivity for human $\alpha 4\beta 2$ ($h\alpha 4\beta 2$) nAChRs over human $\alpha 3\beta 4$ ($h\alpha 3\beta 4$) nAChRs. As one of the main subtypes expressed in the central nervous system (CNS), $h\alpha 4\beta 2$ nAChRs have been implicated in various brain diseases and disorders (e.g., nicotine addiction, anxiety, and depression).^{8–12} On the other hand, $h\alpha 3\beta 4$ nAChR is largely expressed in the peripheral autonomic ganglia where it modulates the release of multiple neurotransmitters. Due to the roles of $h\alpha 3\beta 4$ nAChR in the autonomic ganglia, activity of nicotinic drugs on this subtype has been postulated to mediate a wide range of autonomic side effects, as exemplified by those reported from usage of the classical autonomic blocker, mecamylamine (e.g., constipation, urinary retention, dilation of the pupils, and postural hypotension).^{1–3} Therefore, with interest in developing safer drugs for CNS application, subtype-selectivity was pursued for the $h\alpha 4\beta 2$ nAChRs over the $h\alpha 3\beta 4$ nAChRs.

In this study, we report the discovery of a novel chemical class of nAChR antagonists that allosterically modulate receptor activity using multiple approaches. As a rational drug design strategy, we utilized knowledge gained from our previous studies^{13–18} by incorporating ligand-based modeling, structure-based modeling, pharmacology, and medicinal chemistry. Previously, our laboratory has identified several classes of novel negative allosteric modulators (NAMs) of nAChRs.^{13–16} Effects of those NAMs were insurmountable with increasing concentrations of the orthosteric agonist, epibatidine, suggesting their non-competitive mechanisms of action. Importantly, some of these NAMs showed selectivity for $h\alpha 4\beta 2$ nAChRs over $h\alpha 3\beta 4$ nAChRs. Utilizing a combination of homology modeling, blind docking, and site-directed mutagenesis, an allosteric binding site where these NAMs bind was also identified.^{16–18} This site is located approximately 10 Å from the orthosteric site at the interface between α and β subunits. Since major amino acid residues comprising this site are located at the β subunit, we named this site the ‘ β subunit site’. The ‘ β subunit site’ is sequentially and structurally diverse among subtypes, which provides an explanation for the relative subtype-selectivity shown with some of the NAMs¹⁷: among residues positioned within the ‘ β subunit site’, Thr58, Ser133, Ser138, Ser142, Phe118, and Ser137 showed reduced sequence conservation (less than 26% amino acid identity across nAChR subunits). Other amino acids (Glu60 and Ser97) that contribute to interactions between ligands and receptors occurring through the ‘ β subunit site’ also share a limited degree of sequence conservation among subunits (amino acid identity of 63% and 39%, respectively).¹⁷ The diversity within the ‘ β subunit site’ and the identification of subtype-selective NAMs acting on this site provide support for our approach of targeting allosteric binding sites to develop selective nAChR antagonists. In this study, the physicochemical properties of NAMs that selectively target $h\alpha 4\beta 2$ nAChRs as well as the biochemical characteristics of their binding sites (i.e., the ‘ β subunit site’) mentioned above were exploited. Utilization of ligand-based and structure-based approaches using the previously obtained knowledge led to the discovery of a lead compound of this study (i.e., Compound 1,

4-(allyloxy)-*N*-(6-methylpyridin-2-yl)benzamide) that acts as a NAM of nAChRs. Furthermore, 26 analogs of compound 1 were either synthesized or purchased to determine the structural features that are relevant for potency and relative selectivity toward nAChRs.

2. Chemistry

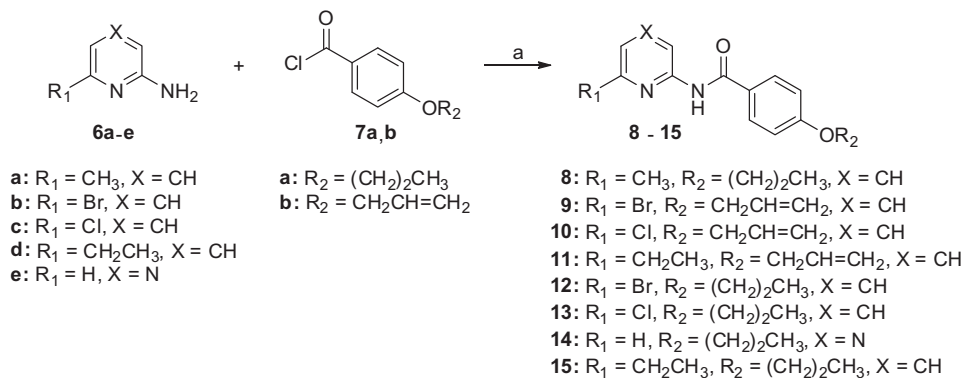
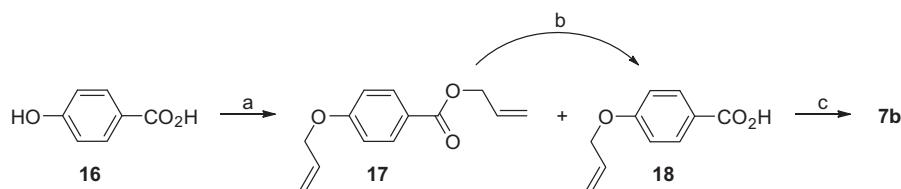
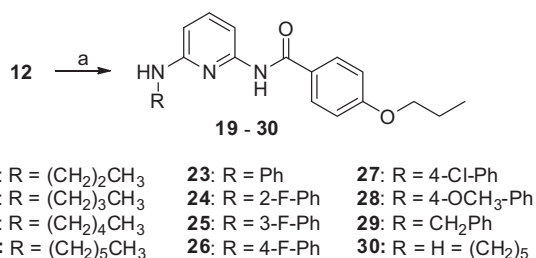
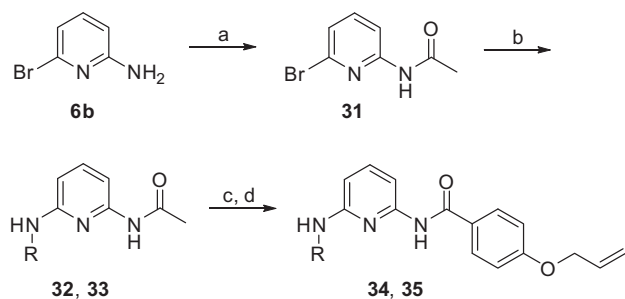
Target compounds 8–15 were obtained through reaction between commercially available 6-substituted-2-aminopyridines 6a–e with 4-propoxybenzoyl chloride (7a) or 4-allyloxybenzoyl chloride (7b) as shown in Scheme 1. Benzoyl chlorides 7a,b were readily prepared by heating 4-propoxybenzoic acid or 4-allyloxybenzoic acid to reflux in thionyl chloride.¹⁹ 4-Allyloxybenzoic acid (18) was made through the reaction between 4-hydroxybenzoic acid (16) and allyl bromide. Since ester 17 was also formed as an undesired side product of the reaction above, 17 was converted to the desired acid 18 by treatment with NaOH in ethanol/water (Scheme 2).

Target compounds 19–30 were synthesized in high yield by reacting a variety of aliphatic and aromatic amines with bromopyridine 12 through Buchwald–Hartwig amination²⁰ (Scheme 3). In contrast, Buchwald–Hartwig reactions using chloropyridine 10 failed to give the desired products. Also, Buchwald–Hartwig coupling using compound 9 as a precursor in an attempt to produce compounds 34 and 35 was unsuccessful, likely due to the presence of the allyl group in 9. An alternative route was thus required to synthesize target compounds 34 and 35. 2-Amino-6-bromopyridine (6b) was first protected by acylation to provide 31, followed by Buchwald–Hartwig amination with either propylamine or butylamine to yield protected alkylaminopyridines 32 and 33, respectively. The acetyl group was removed by treatment with sodium hydroxide, followed by acylation of the resulting primary aromatic amines with 7b to afford target compounds 34 and 35 (Scheme 4).

3. Results

3.1. Pharmacophore and ligand-based virtual screening

In order to identify novel chemical entities that exhibit subtype-selectivity, information obtained from our previous studies was utilized.^{13–18} Four NAMs (i.e., KAB-18, DDR-5, DDR-13, and DDR-18) previously identified by our laboratory¹⁶ were selected based on their preference for $h\alpha 4\beta 2$ nAChRs against $h\alpha 3\beta 4$ nAChRs and used here to generate an initial pharmacophore (Fig. 1). In parallel, structure-based virtual screening (SBVS) using the allosteric binding sites for these four NAMs (i.e., β subunit site) was performed and led to the identification of four novel scaffolds that inhibit the activity of nAChRs with relative selectivity for $h\alpha 4\beta 2$ nAChRs.¹⁴ Among top hits from this SBVS, Hit 2 ((5-amino-*N*-(6-methylpyridin-2-yl)-2-(piperidin-1-yl)benzamide) shares structural similarities with the four NAMs used to generate the initial pharmacophore (Fig. 1). In addition, Hit 2 has lower molecular weight by lacking the substitutions linked to the piperidine ring and thereby possesses potential to exhibit improved bioavailability (Fig. 1). As Hit 2 shows a preference for $h\alpha 4\beta 2$ nAChRs, shares structural similarity with the four NAMs used for initial pharmacophore development, and possesses more desirable drug properties with regard to in vivo bioavailability, the initial pharmacophore was then refined here using Hit 2 from the SBVS. The refined pharmacophore reported here features three hydrophobic regions (HYD1, HYD2, and HYD3) and one hydrogen bond acceptor (HBA) (Fig. 2). This refined pharmacophore model was utilized for ligand-based virtual screening (LBVS) as described below.

Scheme 1. Reagents: (a) DCM, Et₃N.Scheme 2. Reagents: (a) NaOH, allyl bromide, H₂O; (b) NaOH, EtOH/H₂O; (c) thionyl chloride.Scheme 3. Reagents: (a) aliphatic or aromatic amine, Pd₂(dba)₃, (*rac*)-BINAP, NaO-*t*-Bu, toluene.Scheme 4. Reagents: (a) acetyl chloride, DCM, Et₃N; (b) Pd₂(dba)₃, (*rac*)-BINAP, NaOH-*t*-Bu, toluene, propylamine or butylamine; (c) NaOH, H₂O; (d) **7b**, DCM, Et₃N.

3.2. Lead compounds

Chembridge's CNS diversity set of small molecules (~10,000) was virtually screened using the refined pharmacophore (Fig. 2) with 220 hits being identified. The hits were ranked based on a query fit (QFIT) score and pharmacological activity of the top 10 hits was evaluated as described in the Section 6 using HEK

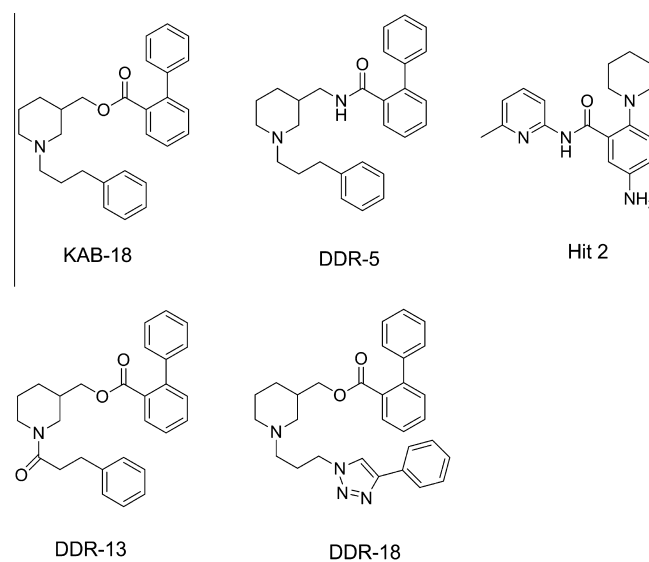


Figure 1. Structures of the compounds used for pharmacophore generation.

tsA201 cells stably expressing either $\alpha 4\beta 2$ nAChRs or $\alpha 3\beta 4$ nAChRs (data not shown). One of the top ranked hits from this LBVS (4-(allyloxy)-*N*-(6-methylpyridin-2-yl)benzamide, **1**) is the focus of this study. As a lead molecule, compound **1** inhibited the activity of $\alpha 4\beta 2$ nAChRs with an IC₅₀ value of 6.0 (3.4–10.6) μM with ~5-fold preference against $\alpha 3\beta 4$ nAChRs (Fig. 3A and B; Table 1). On the other hand, compound **8** (4-(6-methylpyridin-2-yl)-4-propoxybenzamide), in which the propene moiety in the alkoxy portion of compound **1** was replaced with the propane moiety, showed no preference for either subtype; compound **8** produced antagonistic activity on both $\alpha 4\beta 2$ and $\alpha 3\beta 4$ nAChRs with IC₅₀ values of 9.5 (3.7–24.1) μM and 11.1 (8.2–15.2) μM , respectively (Fig. 3A and C; Table 1). Based on their potency and/or selectivity, compounds **1** and **8** were selected as lead molecules

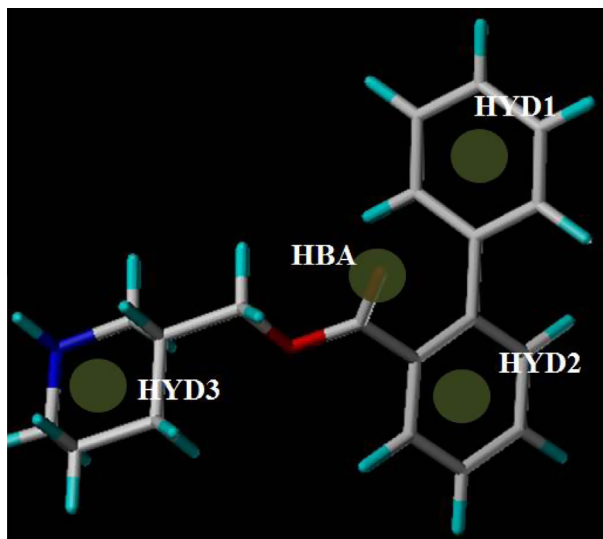


Figure 2. Proposed pharmacophore describing features of subtype selective NAMs of nAChRs. The features of the pharmacophore model generated using GASP are illustrated. Three hydrophobic (HYD1, HYD2, and HYD3) and a hydrogen bonding acceptor (HBA1) feature of the pharmacophore are marked. This pharmacophore was developed as described in the Section 6.

and structural modifications were made at the pyridyl or alkoxy portions of these compounds as outlined in the chemistry section (Fig. 3A). Analyses of structure activity relationship (SAR) studies with 25 analogs of these lead compounds were then performed to determine how modifications are related to the compounds' activity on nAChRs. None of the compounds reported here exhibited agonist activity on either $\alpha 4\beta 2$ or $\alpha 3\beta 4$ nAChRs (Data not

shown). With regard to their mechanisms of action, effects of compounds **1** and **8** were not surmountable with increasing concentrations of epibatidine but led to a decrease in the maximum effect of epibatidine (Fig. 4). This suggested that compounds **1** and **8** are not competing with epibatidine for the orthosteric binding site but instead act as non-competitive antagonists of nAChRs.

3.3. Analyses of SAR studies on analogs of compound 1

In the first series of SAR studies, chemical modifications were made primarily to the alkoxy portion of the lead molecule, compound **1**, to determine functional effects of those structural changes. Concerning modifications in the alkoxy portion of compound **1**, replacement of the propene group with propane moiety (compound **8**) resulted in an increase in potency on $\alpha 3\beta 4$ nAChRs with no change in potency on $\alpha 4\beta 2$ nAChRs; thus, this modification led to loss of relative selectivity for $\alpha 4\beta 2$ nAChRs (Table 1). Introduction of a methyl moiety (compound **2**) and replacement of the propene with a propyne (compound **3**) induced changes in functional activity on nAChR in a subtype-specific manner. While those changes led to decreases in potency on $\alpha 4\beta 2$ nAChRs, the same changes resulted in a trend to increased potency on $\alpha 3\beta 4$ nAChRs. However, the increases in potency were not statistically significant (compound **1** vs **2**, $p = 0.261$; compound **1** vs **3**, $p = 0.143$). Compound **4** had structural modifications on both the pyridyl and alkoxy portions of compound **1**; a methyl group was introduced to the methylpyridine in the pyridyl portion and the propene moiety in the alkoxy portion was replaced by an ethyl residue. These modifications led to a decrease in potency on $\alpha 4\beta 2$ nAChRs, whereas they caused an increase in potency on $\alpha 3\beta 4$ nAChRs. Overall, these structural changes decreased the selectivity ratio and compound **4** inhibited the activity of $\alpha 4\beta 2$ and $\alpha 3\beta 4$ nAChRs with comparable potency. The pyridyl portion of

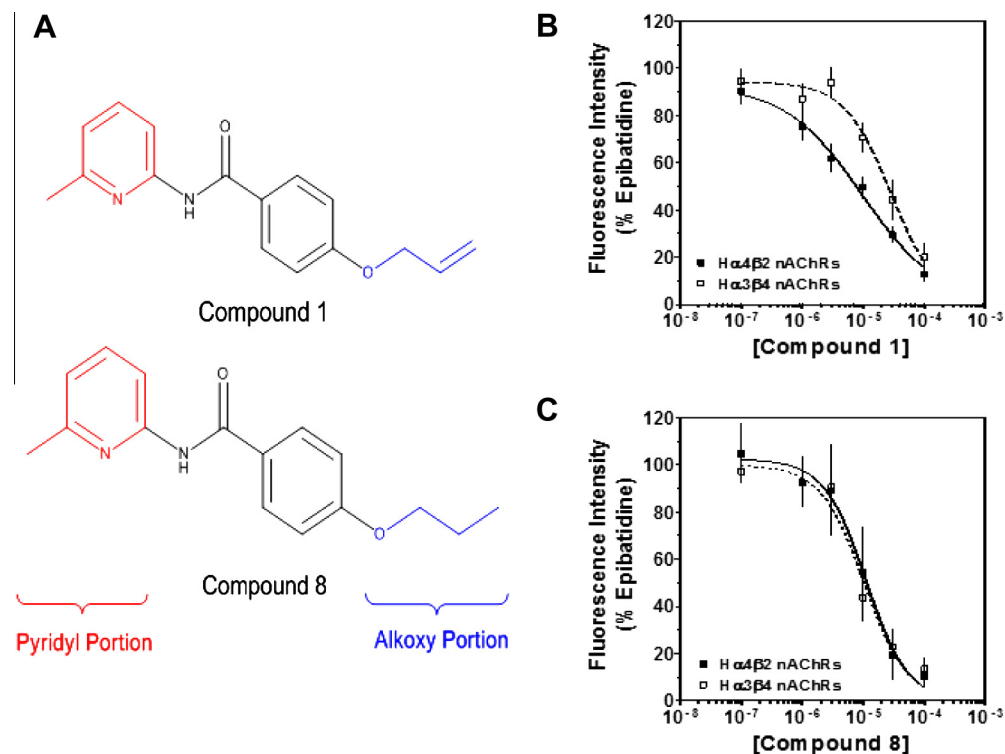
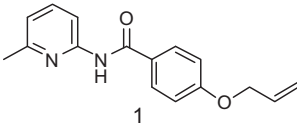
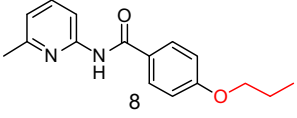
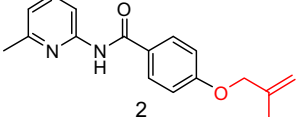
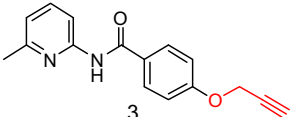
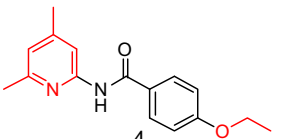
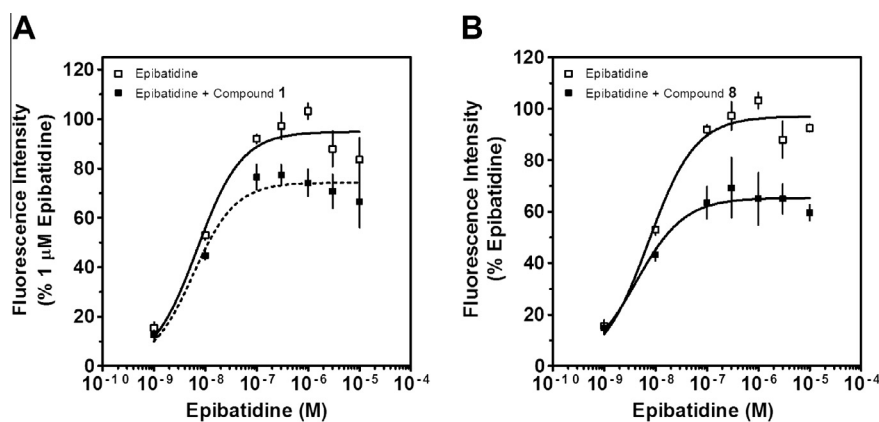


Figure 3. Concentration–response effects of compounds **1** and **8** on $\alpha 4\beta 2$ nAChRs and $\alpha 3\beta 4$ nAChRs. (A) Structure of lead compounds **1** and **8** with the location of the primary substitutions for SAR studies. The concentration–response effects of compound **1** (B) and **8** (C) were investigated on $\alpha 4\beta 2$ nAChRs (■) and $\alpha 3\beta 4$ nAChRs (□) as described in the Section 6. Values represent means \pm SEMs ($n = 4–7$). Data are reported as a percentage of peak fluorescence responses for $1 \mu\text{M}$ epibatidine. IC_{50} values of compounds **1** and **8** are reported in Table 1.

Table 1
SAR studies on the alkoxy portion of Compound 1

Compound	h α 4 β 2 nAChRs		h α 3 β 4 nAChRs		Selectivity ^c
	IC ₅₀ value ^a (μ M)	n_h ^b	IC ₅₀ value ^a (μ M)	n_h ^b	
	6.0 (3.4–10.6)	–0.7	31.7 (22.8–44.0)	–1.1	5.3
	9.5 (3.7–24.1)	–1.6	11.1 (8.2–15.2)	–1.5	1.2
	19.6 (16.1–23.9)	–1.0	24.7 (17.8–33.9)	–1.5	1.3
	19.4 (15.7–24.0)	–1.1	21.7 (15.3–31.0)	–1.6	1.1
	17.1 (11.2–26.0)	–0.9	17.4 (14.9–20.4)	–0.8	1.0

^a Values represent geometric means (confidence limits), $n = 5$ –10.^b n_h , Hill coefficient.^c Selectivity; fold ratio of IC₅₀-h α 3 α 4 β nAChRs/IC₅₀-h α 4 β 2 nAChRs.**Figure 4.** Concentration–response effects of epibatidine in the absence and presence of compounds 1 and 8. The concentration–response effects of epibatidine were investigated in the absence (□) and the presence (■) of compounds 1 (A) and 8 (B) on human α 4 β 2 nAChRs, using calcium accumulation assays described in the Section 6. Values represent means \pm SEM ($n = 4$).

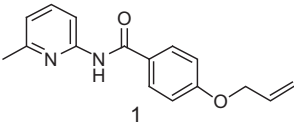
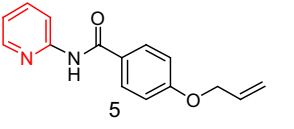
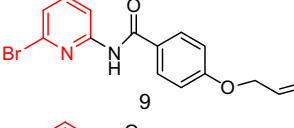
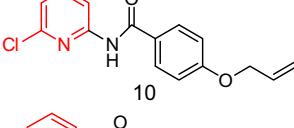
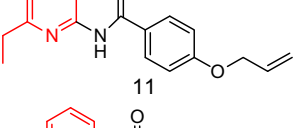
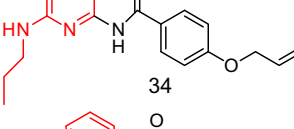
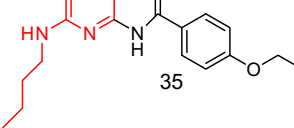
compound 1 was also modified using several different substitutions and functional effects of those changes were investigated (Table 2). Replacement of 2-methylpyridine with pyridine (compound 5) caused decreases in potency for both h α 4 β 2 and h α 3 β 4 nAChRs. Compound 5 still maintained relative selectivity for h α 4 β 2, although the selectivity ratio decreased to \sim 3-fold. The introduction of halogen atoms (e.g., chlorine and bromine) led to decreases in potency on both h α 4 β 2 and h α 3 β 4 nAChRs. Bromine addition (compound 9) resulted in \sim 11-fold and \sim 2-fold decreases in potency on h α 4 β 2 and h α 3 β 4 nAChRs, respectively, while the chlorinated analog 10 showed no activity up to 100 μ M on both subtypes. Replacement of 2-methylpyridine with 2-ethylpyridine

(compound 11) led to a decrease in potency on h α 4 β 2 nAChRs. However, potency on h α 3 β 4 nAChRs was not affected by this substitution, leading to a decrease in the selectivity ratio. On the other hand, replacement of 2-methylpyridine with *N*-propylpyridin-2-amine (compound 34) or *N*-butylpyridin-2-amine (compound 35) resulted in decreases in potency on h α 4 β 2 nAChRs and slight increases in potency on h α 3 β 4 nAChRs.

3.4. Analyses of SAR studies on analogs of compound 8

In the second series of SAR studies, compound 8 was used as the basis of comparison and functional effects of different substitutions

Table 2
SAR studies on the pyridyl portion of Compound **1**

Compound	h α 4 β 2 nAChRs		h α 3 β 4 nAChRs		Selectivity ^c
	IC ₅₀ value ^a (μ M)	n_h ^b	IC ₅₀ value ^a (μ M)	n_h ^b	
 1	6.0 (3.4–10.6)	–0.7	31.7 (22.8–44.0)	–1.1	5.3
 5	19.3 (14.5–25.7)	–1.0	61.4 (40.6–92.8)	–1.3	3.2
 9	70.1 (53.9–91.2)	–1.1	65.5 (54.4–78.9)	–0.9	0.9
 10	>100 ^d	\sim^e	>100 ^d	\sim^e	\sim^e
 11	20.5 (15.5–27.3)	–1.3	27.4 (14.6–51.2)	–0.9	1.3
 34	14.8 (10.6–20.8)	–2	11.7 (8.2–16.8)	–2.1	0.8
 35	22.4 (12.4–40.4)	–1.6	19.2 (13.7–26.9)	–1.7	0.9

^a Values represent geometric means (confidence limits), $n = 5$ –10.

^b n_h , Hill coefficient.

^c Selectivity; fold ratio of IC₅₀-h α 3 β 4 nAChRs/IC₅₀-h α 4 β 2 nAChRs.

^d No activity up to 100 μ M.

^e Could not be determined.

on the pyridyl portion of compound **8** were explored (Table 3). Similar to the SAR studies on compound **1**, introduction of halogen atoms to the pyridyl portion of compound **8** produced significant decreases in potency for both subtypes. Analogs with bromine or chlorine substitutions (compounds **12** and **13**) either showed weak inhibitory activity (IC₅₀ >50 μ M) or no effects up to 100 μ M on both subtypes. Replacement of 2-methylpyridine with pyrazine (compound **14**) resulted in a \sim 3-fold decrease in potency on h α 4 β 2 nAChRs and a \sim 2-fold decrease in potency on h α 3 β 4 nAChRs. Substitution of 2-ethylpyridine at the pyridyl portion of compound **8** (compound **15**) led to \sim 5-fold and \sim 2-fold decreases in potency on h α 4 β 2 and h α 3 β 4 nAChRs, respectively. Four analogs that have different alkylamine substitutions at the pyridine ring (compounds **19**–**22**) provided insight into the functional effects of chain length on the pyridyl portion of compound **8**. Analogs incorporating longer alkylamine side chains showed lower potency on both h α 4 β 2 and h α 3 β 4 nAChRs, suggesting inverse correlation between the chain length and potency. Introduction of structurally bulky groups to the pyridine ring led to loss of activity on both h α 4 β 2 and h α 3 β 4 nAChRs (compounds **23**–**30**).

4. Discussion

Computer aided drug discovery (CADD) has become an increasingly useful tool to facilitate many steps of the drug discovery process such as identifying hits, enabling de novo design of ligands, and modeling ADMET (absorption, distribution, metabolism, excretion, and toxicity) properties.^{21–23} In particular, virtual screening (VS) has been widely used to guide lead identification by employing various statistical analyses and algorithms designed to search large chemical libraries in silico.²⁴ Ligand-based virtual screening (LBVS) takes advantage of available information for known ligands such as structures, shape of individual fragments, and electrostatic properties; whereas SBVS exploits the knowledge of the structure of the target protein.^{25,26} In this study, a novel scaffold (compound **1**) was identified through a virtual screening, using ligand-based and structure-based approaches. Previously, our laboratory identified NAMs (i.e., KAB-18, DDR-5, DDR-13, and DDR-18) that showed relative selectivity for h α 4 β 2 nAChRs against h α 3 β 4 nAChRs (Fig. 1).¹⁶ Furthermore, a combination of homology modeling, blind docking, and site-directed mutagenesis identified the β subunit

Table 3
SAR studies on the pyridyl portion of Compound **8**

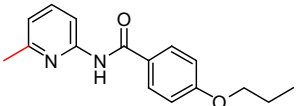
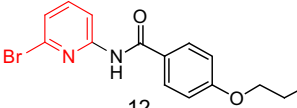
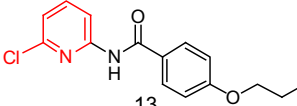
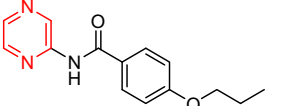
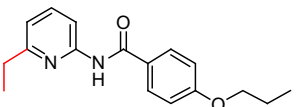
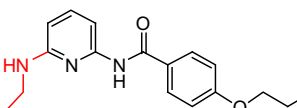
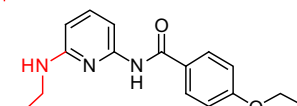
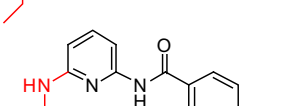
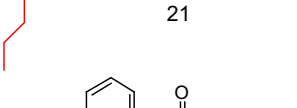
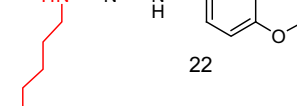
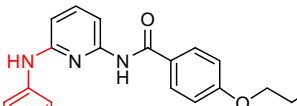
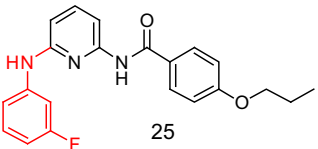
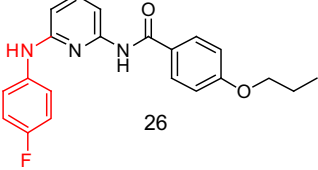
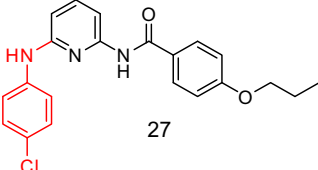
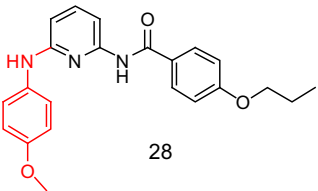
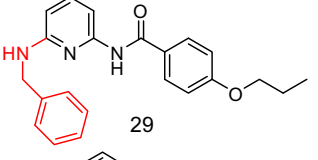
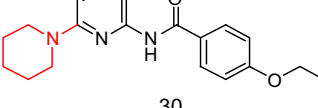
Compound	h α 4 β 2 nAChRs		h α 3 β 4 nAChRs		Selectivity ^c
	IC ₅₀ value ^a (μ M)	n _h ^b	IC ₅₀ value ^a (μ M)	n _h ^b	
 8	7.5 (3.6–15.5)	–1.3	11.5 (8.0–15.2)	–0.8	1.5
 12	80.7 (49.3–132.0)	–1.0	>100 ^d	~ ^e	~ ^e
 13	>100 ^d	~ ^e	>100 ^d	~ ^e	~ ^e
 14	23.2 (16.4–32.6)	–1.2	22.5 (12.0–42.0)	–0.9	1.0
 15	37.6 (22.6–62.7)	–1.7	29.2 (27.1–31.5)	–1.6	0.8
 19	15.4 (10.5–22.6)	–1.4	12.6 (6.4–24.6)	–1.1	0.8
 20	54.1 (24.7–118.0)	–0.8	77.8 (42.2–143.0)	–0.7	1.4
 21	>100 ^d	~ ^e	>100 ^d	~ ^e	~ ^e
 22	>100 ^d	~ ^e	>100 ^d	~ ^e	~ ^e
 23	>100 ^d	~ ^e	>100 ^d	~ ^e	~ ^e
 24	>100 ^d	~ ^e	>100 ^d	~ ^e	~ ^e

Table 3 (continued)

Compound	h α 4 β 2 nAChRs		h α 3 β 4 nAChRs		Selectivity ^c
	IC ₅₀ value ^a (μ M)	n_h ^b	IC ₅₀ value ^a (μ M)	n_h ^b	
 25	>100 ^d	\sim^e	>100 ^d	\sim^e	\sim^e
 26	>100 ^d	\sim^e	>100 ^d	\sim^e	\sim^e
 27	>100 ^d	\sim^e	>100 ^d	\sim^e	\sim^e
 28	>100 ^d	\sim^e	>100 ^d	\sim^e	\sim^e
 29	>100 ^d	\sim^e	>100 ^d	\sim^e	\sim^e
 30	>100 ^d	\sim^e	>100 ^d	\sim^e	\sim^e

^a Values represent geometric means (confidence limits), $n = 5-10$.

^b n_h , Hill coefficient.

^c Selectivity; fold ratio of IC₅₀-h α 3 β 4 nAChRs/IC₅₀-h α 4 β 2 nAChRs.

^d No activity up to 100 μ M.

^e Could not be determined.

site', a novel allosteric binding site on the receptor where these NAMs interact.¹⁶⁻¹⁸ In contrast to the orthosteric binding site, the ' β subunit site' showed reduced sequence conservation. The ' β subunit site' was then used for SBVS with a hypothesis that its sequential and structural diversity could provide molecular foundations to develop selective nAChR drugs. Supporting this hypothesis, hits from this SBVS showed preference for h α 4 β 2 nAChRs.¹⁴ Interestingly, one of the hits from the SBVS, (5-amino-*N*-(6-methylpyridin-2-yl)-2-(piperidin-1-yl)benzamide; Hit 2) shares the following structural features with the previously identified four subtype-selective NAMs (Fig. 1): (1) The carbonyl group is attached to the aryl ring and (2) the aryl ring has a six-membered ring at the *ortho* position. In order to identify a novel chemical scaffold with relative selectivity for h α 4 β 2 nAChRs, the above mentioned information obtained from the previous studies was utilized. Initially, chemical and structural features of four subtype-selective NAMs (i.e., KAB-18, DDR-5, DDR-13, and DDR-18) were used to generate a pharmacophore. This initial pharmacophore was then refined

using the structure of Hit 2, one of the hits from SBVS¹⁴, as it (1) shows relative selectivity for h α 4 β 2 nAChRs over h α 3 β 4 nAChRs, (2) displays structural similarity to the four NAMs used to develop the initial pharmacophore, and (3) has physicochemical properties associated with more desirable ADMET properties. The refined pharmacophore was subsequently applied to the LBVS and led to the identification of compound 1, a lead molecule of this study. In particular, with an aim of developing CNS applicable drugs, we performed the LBVS using the Chembridge's CNS diversity set. Molecules contained in this library generally possess favorable physicochemical properties with regard to CNS bioavailability due to multiple strict sets of property filters. However, the strict criteria for drug-like properties result in the small-sized library with decreased molecular diversity. This might have limited the potential of identifying more potent and/or selective drugs, as well as chemical diversity of hit molecules.

In the present study, we used HEK tsA201 cells stably expressing h α 4 β 2 or h α 3 β 4 nAChRs for pharmacological evaluations of the

analogs. As reported in our previous paper, pharmacological properties of classical agonists (epibatidine and nicotine) and antagonists (mecamylamine and d-tubocurarine) determined using these cells lines are in good agreement with previously reported values.¹⁶ In particular, the non-competitive nAChR antagonist mecamylamine showed inhibitory activity with IC₅₀ values of 0.6 μM and 0.7 μM on hα4β2 nAChRs and hα3β4 nAChRs, respectively. The competitive antagonist d-tubocurarine displayed antagonist activity with IC₅₀ values of 9.2 and 6.8 μM on hα4β2 nAChRs and hα3β4 nAChRs, respectively. Unlike these non-selective nAChR antagonists, the lead molecule (compound **1**) exhibited hα4β2 nAChR-selective antagonism. Compound **1** showed antagonistic activity with an IC₅₀ value of 6.0 (3.4–10.6) μM on hα4β2 nAChRs with ~5-fold preference against hα3β4 nAChRs (Table 1). Its non-competitive mechanism of action was described by a decrease in maximum effects of the orthosteric ligand epibatidine (Fig. 4A).

In order to determine effects of structural modifications to the pyridyl or alkoxy portions of the molecules with regard to their functional activities, analyses of the SAR studies on analogs of compounds **1** and **8** were performed. The most significant finding from the SAR studies of analogs of compound **1** is that modification of propene to propane (compound **1** vs compound **8**) led to loss of preference for hα4β2, suggesting the importance of a double bond in the alkoxy portion of the molecules with regard to subtype-selectivity. Another analog containing the propene moiety (compound **5**) also exhibited ~3-fold preference for hα4β2 nAChRs against hα3β4 nAChRs. However, relative selectivity for hα4β2 nAChRs was not observed for other analogs that also have the propene moiety (compounds **9–11**, **34**, and **35**). Introduction of halogen atoms, an ethyl moiety, and alkyl amines (compounds **9–11**, **34**, and **35**) to the pyridyl portion of the molecules abolished the subtype-selectivity. Comparison with their counterparts containing the propane moiety (compounds **12**, **13**, and **15**) suggested that functional activities were mainly determined by the pyridyl portion of the molecules for this series of compounds and modification of propene to propane did not affect either potency or subtype-selectivity. Structural modifications to both the pyridyl and alkoxy portions of the molecules led to an analog (compound **4**) that has comparable potency on hα4β2 and hα3β4 nAChRs. Collectively, these data suggest that both portions of the molecules contribute to the selectivity for hα4β2 nAChRs.

The SAR studies on analogs of compound **8** also provide insight into the functional effects of chemical modifications on the pyridyl portion of the molecules. With the aim of exploring the appropriate chain length linked to the pyridine ring, a series of compounds (compounds **8**, and **19–22**) were synthesized. SAR studies on these compounds suggested that steric hindrance exists at the portion of the receptor-binding pocket where the pyridine moiety interacts. Increasing the chain length resulted in decreases in potency for both subtypes. Similarly, substitutions with structurally bulky moieties to the pyridine ring (compounds **23–30**) led to loss of activity on both subtypes.

5. Conclusion

For the past several years, our laboratory has focused on discovering small molecules that modulate nAChR activity with several chemical classes of ligands being reported.^{13–18,27–29} Here, we described the identification of a novel chemical class of NAMs of nAChRs through the application of multiple approaches. Iterative cycles of virtual screening using ligand-based and structure-based approaches led to the identification of the lead molecule, compound **1** (4-(allyloxy)-N-(6-methylpyridin-2-yl)benzamide). As the lead, compound **1** inhibits the activity of hα4β2 nAChRs with ~5-fold preference against hα3β4 nAChRs. To gain insight into

the chemical/structural properties of the molecules pertaining to antagonistic activity on nAChRs, we have obtained 27 benzamide analogs and performed SAR studies on these analogs. It is notable that among the 27 analogs, two analogs (i.e., compounds **1** and **5**) exhibit preference for hα4β2 nAChRs, although the selectivity ratios remain modest.

The study described here documents the successful utilization of a multifaceted approach for rational drug discovery employing computational modeling, pharmacology, and medicinal chemistry, which has led to the identification of a novel chemical class of nAChR NAMs including molecules that show relative selectivity for hα4β2 nAChRs. The discovery of subtype-selective NAMs of nAChRs described here should contribute significantly to our understanding of the involvement of specific nAChR subtypes in normal and pathophysiological states and may hold clinical promise for diseases linked to nAChRs.

6. Experimental

6.1. Materials

The calcium sensitive fluorescent probe, Calcium 5 NW dye, was obtained from Molecular Devices (Sunnyvale, CA). Dulbecco's Modified Eagle Medium (DMEM), penicillin, streptomycin and L-glutamine were purchased from Invitrogen Corporation (Grand Island, NY). The nAChR agonist, epibatidine was obtained from Sigma–Aldrich (St. Louis, MO). All other reagents were obtained from Fisher Scientific (Pittsburg, PA).

6.2. Pharmacophore generation

A pharmacophore model was generated using a procedure previously reported by our laboratory.^{16,30} The four NAMs (i.e. KAB-18, DDR-5, DDR-13, and DDR-18) that selectively target hα4β2 nAChRs were aligned using GASP (Genetic Algorithm Similarity Program, SYBYL 7.1) with default settings (population size, 125; the allele mutate weight, 96; the fitness increment, 0.02). Alignments for each set of molecules were repeated for 10 runs, followed by the optimal model selection through visual inspection. This initial pharmacophore model was then refined through observations of a novel chemical structure identified by SBVS.¹⁴ One of the hits from this SBVS contained three of the four hydrophobic pharmacophore elements. Therefore, a hydrophobic domain of the initial pharmacophore was eliminated using the 'edit pharmacophore' option in SYBYL 7.1.

6.3. Ligand-based virtual screening

Ligand-based virtual screening (LBVS) was performed with the above-mentioned pharmacophore. Chembridge's CNS diversity set of small molecules (~10,000) was virtually explored with an aim of identifying molecules that contain chemical and geometrical descriptors defined by the pharmacophore model. The LBVS was performed with UNITY (SYBYL 7.1), using the default settings of FlexX (the 3D dynamic setting) search options. In order to maximize the diversity in molecular scaffolds, the LBVS was performed with Lipinski filter turned 'off'. The hits were then scored in UNITY based on their ability to fit the spatial and chemical features described by the pharmacophore.

6.4. Calcium accumulation assay

For pharmacological evaluation of the synthesized analogs, calcium accumulation assay was performed with HEK tsA201 cells stably expressing either hα4β2 nAChRs or hα3β4 nAChRs (obtained from Professor Jon Lindstrom, University of Pennsylvania,

Philadelphia, PA), using a procedure previously reported by our laboratory.¹³ Briefly, cells were plated 24 h prior to experiments in clear pre-coated 96-well culture plates. Plates were incubated at 37 °C in 5% CO₂ in supplemented Dulbecco's modified Eagle's medium and cells were allowed to form a ~100% confluent monolayer (typically 24 h after plating). On the day of the experiment, cells were washed (100 µL) with HEPES-buffered Krebs (HBK) solution and incubated for 1 hour at room temperature with 50% Calcium 5 NW dye (Molecular Devices). The plates were then placed into a fluid handling integrated fluorescence plate reader (FlexStation II, Molecular Devices, Sunnyvale, CA) and treatment solutions were added to the cells. Changes in intracellular calcium levels were then simultaneously measured at excitation of 485 nm and emission of 525 nm from the bottom of the plate every 1.5 s. For each drug, six concentrations (0.1–100 µM) were used to generate full concentration–response curves and results are reported as the concentration of drugs that reduced the effect of the 1 µM epibatidine control by 50% (IC₅₀ values). All compounds were initially dissolved with 100% DMSO (0.01 M stocks) and further dilutions were made in HEPES-buffered Krebs (HBK) solution (≤100 µM). The DMSO concentration at this compound concentration was less than 1% and had no effects on basal or agonist-induced increases in fluorescence intensity.¹⁶ Due to solubility problems, compound concentrations greater than 100 µM were not used in our concentration–response studies.

6.5. Calculations

Quantification of functional response was performed by determining the ability of compounds to inhibit the fluorescence signal increases in response to epibatidine (1 µM). Curve fitting was performed by Prism software (GraphPad, San Diego, CA) using the equation for a single-site sigmoidal dose–response curve with a variable slope. Functional data were calculated from the number of observations (*n*) performed in triplicate. IC₅₀ values are expressed as geometric means (95% confidence limits) of each experiment. The Hill coefficients (*n_h*) represented in the table were calculated by taking arithmetic mean of each Hill coefficient from individual experiments.

6.6. General procedure for the preparation of compounds

6.6.1. General experimental

¹H NMR (300 MHz) and ¹³C NMR (75 MHz) spectra were recorded on a Bruker 300 UltraShield spectrometer. Electrospray ionization mass spectrometry (ESI-MS) was performed by The Ohio State University Mass Spectrometry and Proteomics Facility. Melting points were measured on a Fisher Scientific melting point apparatus and were not corrected. Gravity and flash column chromatography were performed using type 60A silica gel (60–230 mesh) from Fisher Scientific. Solid compounds were further purified by recrystallization. Elemental analyses, performed by Atlantic Microlabs, Norcross, GA, were carried out for all compounds prepared in our lab displaying an IC₅₀ value of <50 µM as well as for other selected target compounds.

6.6.2. Materials

All chemicals and solvents were purchased from Aldrich Chemical Co., TCI, Alfa Aesar, Fisher Scientific, or Matrix Scientific and were used without further purification. Compounds **1–5** were purchased from Chembridge (San Diego, CA). These compounds were obtained at ≥90% purity as determined by ¹H NMR analyses as stated by the supplier. Compounds prepared in our lab were characterized as free bases unless otherwise stated, but all were tested as hydrochloric acid salts in the bioassay to aid in solubilizing the compounds in the biological assay buffer.

6.6.3. Preparation and characterization of compounds

6.6.3.1. *N*-(6-Methylpyridin-2-yl)-4-propoxybenzamide (8). A mixture of 2-amino-6-methylpyridine (**6a**) (0.61 g, 5.6 mmol) and triethylamine (4 mL) in dichloromethane (DCM) (10 mL) was added dropwise to freshly made 4-propoxybenzoyl chloride (**7a**) (1.19 g, 6.0 mmol) in DCM (5 mL) and the reaction mixture was heated to reflux overnight. After cooling, the mixture was washed with water, brine and dried with anhydrous MgSO₄. The solvent was evaporated under reduced pressure, then the crude product was further purified on a silica gel column using hexanes/ethyl acetate (3:1) to yield the pure product (1.2 g, 79%) as a colorless solid, mp 86–89 °C. ¹H NMR (CDCl₃, 300 MHz) δ 8.59 (s, 1H), 8.19 (d, *J* = 8.1 Hz, 1H), 7.89 (d, *J* = 8.4 Hz, 2H), 7.64 (dd, *J* = 7.8 Hz, 1H), 6.96 (d, *J* = 8.4 Hz, 2H), 6.91 (d, *J* = 7.5 Hz, 1H), 3.99 (t, *J* = 6.6 Hz, 2H), 2.46 (s, 3H), 1.85 (m, 2H), 1.06 (t, *J* = 7.2 Hz, 3H); ¹³C NMR (CDCl₃, 75 MHz) δ 165.2, 162.4, 156.8, 151.1, 138.7, 129.1, 126.3, 119.2, 114.4, 110.9, 69.7, 24.0, 22.5, 10.5; ESI-MS *m/z* 271.11 (M+H, 100); Anal. Calcd for C₁₆H₁₈N₂O₂ (270.14): C, 71.09; H, 6.71; N, 10.36. Found: C, 70.71; H, 6.78; N, 10.06.

6.6.3.2. 4-(Allyloxy)-*N*-(6-bromopyridin-2-yl)benzamide (9). The reaction was similar to the one above employing 2-amino-6-bromopyridine (**6b**) (233 mg, 1.35 mmol) and 4-allyloxybenzoyl chloride (**7b**) (265 mg, 1.35 mmol) to yield **9** (367 mg, 82%). Purification was carried out on a silica gel column using hexanes/ethyl acetate (4:1) to provide the pure compound as a colorless solid, mp 102–105 °C. ¹H NMR (CDCl₃, 300 MHz) δ 8.52 (s, 1H), 8.35 (d, *J* = 8.4 Hz, 1H), 7.88 (d, *J* = 8.7 Hz, 2H), 7.60 (dd, *J* = 8.1 Hz, 1H), 7.24 (d, *J* = 7.8 Hz, 1H), 7.00 (d, *J* = 9.0 Hz, 2H), 6.07 (m, 1H), 5.45 (d, *J* = 17.4 Hz, 1H), 5.34 (d, *J* = 10.5 Hz, 1H), 4.62 (d, *J* = 5.1 Hz, 2H); ¹³C NMR (CDCl₃, 75 MHz) δ 165.0, 162.1, 151.8, 140.7, 139.3, 132.4, 129.2, 125.9, 123.4, 118.3, 114.8, 112.4, 69.0; ESI-MS *m/z* 333.02 (M+H, 68).

6.6.3.3. 4-(Allyloxy)-*N*-(6-chloropyridin-2-yl)benzamide (10).

The reaction was similar to the one above employing 2-amino-6-chloropyridine (**6c**) (60 mg, 0.47 mmol) and 4-allyloxybenzoyl chloride (**7b**) (67 mg, 0.34 mmol) to yield **10** (85 mg, 87%). Purification was carried out on a silica gel column using hexanes/ethyl acetate (3:1) to provide the pure compound as a colorless solid, mp 98–100 °C. ¹H NMR (CDCl₃, 300 MHz) δ 8.48 (s, 1H), 8.33 (d, *J* = 7.8 Hz, 1H), 7.89 (d, *J* = 9.0 Hz, 2H), 7.73 (dd, *J* = 7.8 Hz, 1H), 7.11 (d, *J* = 7.2 Hz, 1H), 7.02 (d, *J* = 8.7 Hz, 2H), 6.07 (m, 1H), 5.46 (d, *J* = 17.4 Hz, 1H), 5.35 (d, *J* = 10.5 Hz, 1H), 4.64 (d, *J* = 5.1 Hz, 2H); ¹³C NMR (CDCl₃, 75 MHz) δ 165.0, 162.1, 151.6, 149.0, 141.0, 132.4, 129.2, 125.9, 119.6, 118.3, 114.9, 112.1, 69.0; ESI-MS *m/z* 311.05 (M+Na, 100).

6.6.3.4. 4-(Allyloxy)-*N*-(6-ethylpyridin-2-yl)benzamide (11).

The reaction was similar to the one above employing 2-amino-6-ethylpyridine (**6d**) (70 mg, 0.57 mmol) and 4-allyloxybenzoyl chloride (**7b**) (112 mg, 0.57 mmol) to yield **11** (143 mg, 89%). Purification was carried out on a silica gel column using hexanes/ethyl acetate (3:1) to provide the pure compound as a colorless solid, mp 42–45 °C. ¹H NMR (CDCl₃, 300 MHz) δ 8.61 (s, 1H), 8.19 (d, *J* = 8.1 Hz, 1H), 7.92 (d, *J* = 8.7 Hz, 2H), 7.67 (dd, *J* = 7.8 Hz, 1H), 6.99 (d, *J* = 8.7 Hz, 2H), 6.93 (d, *J* = 7.5 Hz, 1H), 6.07 (m, 1H), 5.44 (d, *J* = 17.4 Hz, 1H), 5.33 (d, *J* = 10.5 Hz, 1H), 4.61 (d, *J* = 5.4 Hz, 2H), 2.73 (q, *J* = 7.5 Hz, 2H), 1.29 (t, *J* = 7.5 Hz, 3H); ¹³C NMR (CDCl₃, 75 MHz) δ 165.1, 162.1, 161.7, 151.0, 138.8, 132.6, 129.2, 126.7, 118.2, 117.9, 114.7, 111.2, 68.9, 31.0, 13.8; ESI-MS *m/z* 283.11 (M+H, 100); Anal. Calcd for C₁₇H₁₈N₂O₂ (282.14): C, 72.32; H, 6.43; N, 9.92. Found: C, 72.36; H, 6.47; N, 9.65.

6.6.3.5. *N*-(6-Bromopyridin-2-yl)-4-propoxybenzamide (12).

The reaction was similar to the one above employing 2-amino-6-bromopyridine (**6b**) (1.25 g, 7.2 mmol) and 4-propoxybenzoyl chloride (**7a**) (1.42 g, 7.2 mmol) to yield **12** (1.96 g, 81%). Purification was carried out on a silica gel column using hexanes/ethyl acetate (3:1) to provide the pure

compound as a colorless solid, mp 128–132 °C. $^1\text{H NMR}$ (CDCl_3 , 300 MHz) δ 8.52 (s, 1H), 8.36 (d, J = 8.1 Hz, 1H), 7.88 (d, J = 8.7 Hz, 2H), 7.61 (dd, J = 8.1 Hz, 1H), 7.25 (d, J = 7.5 Hz, 1H), 7.00 (d, J = 8.7 Hz, 2H), 4.00 (t, J = 6.6 Hz, 2H), 1.86 (m, 2H), 1.07 (t, J = 7.5 Hz, 3H); $^{13}\text{C NMR}$ (CDCl_3 , 75 MHz) δ 165.1, 162.7, 151.8, 140.7, 139.2, 129.2, 125.5, 123.4, 114.6, 112.4, 69.8, 22.5, 10.5; ESI-MS m/z 357.02 (M+Na, 100), 335.04 (M+H, 39).

6.6.3.6. *N*-(6-Chloropyridin-2-yl)-4-propoxybenzamide (13). The reaction was similar to the one above employing 2-amino-6-chloropyridine (**6c**) (1.6 g, 12.5 mmol) and 4-propoxybenzoyl chloride (**7a**) (3.3 g, 16.7 mmol) to yield **13** (3.05 g, 84%). Purification was carried out on a silica gel column using hexanes/ethyl acetate (3:1) to provide the pure compound as colorless solid, mp 123–125 °C. $^1\text{H NMR}$ (CDCl_3 , 300 MHz) δ 8.48 (s, 1H), 8.33 (d, J = 8.1 Hz, 1H), 7.88 (d, J = 9.0 Hz, 2H), 7.72 (dd, J = 8.1 Hz, 1H), 7.10 (d, J = 7.8 Hz, 1H), 6.99 (d, J = 8.7 Hz, 2H), 4.01 (t, J = 6.6 Hz, 2H), 1.86 (m, 2H), 1.08 (t, J = 7.5 Hz, 3H); $^{13}\text{C NMR}$ (CDCl_3 , 75 MHz) δ 165.1, 162.7, 151.6, 148.9, 141.0, 129.2, 125.5, 119.6, 114.6, 112.1, 69.8, 22.5, 10.5; ESI-MS m/z 313.06 (M+Na, 100).

6.6.3.7. 4-Propoxy-*N*-(pyrazin-2-yl)benzamide (14). The reaction was similar to the one above employing 2-aminopyrazine (**6e**) (278 mg, 2.93 mmol) and 4-propoxybenzoyl chloride (**7a**) (582 mg, 2.93 mmol) to yield **14** (127 mg, 17%). Purification was carried out on a silica gel column using hexanes/ethyl acetate (3:1) to provide the pure compound as a colorless solid, mp 137–140 °C. $^1\text{H NMR}$ (CDCl_3 , 300 MHz) δ 9.73 (s, 1H), 8.57 (br, 1H), 8.38 (d, J = 2.4 Hz, 1H), 8.27 (br, 1H), 7.92 (d, J = 8.8 Hz, 2H), 7.01 (d, J = 8.8 Hz, 2H), 4.02 (t, J = 6.6 Hz, 2H), 1.87 (m, 2H), 1.08 (t, J = 7.2 Hz, 3H); $^{13}\text{C NMR}$ (CDCl_3 , 75 MHz) δ 164.9, 162.8, 148.5, 142.0, 140.1, 137.2, 129.4, 125.1, 114.7, 69.8, 22.5, 10.5; ESI-MS m/z 258.10 (M + H, 100); Anal. Calcd for $\text{C}_{14}\text{H}_{15}\text{N}_3\text{O}_2$ (257.12): C, 65.35; H, 5.88; N, 16.33. Found: C, 65.01; H, 5.90; N, 15.95.

6.6.3.8. *N*-(6-Ethylpyridin-2-yl)-4-propoxybenzamide (15). The reaction was similar to the one above employing 2-amino-6-ethylpyridine (**6d**) (350 mg, 2.87 mmol) and 4-propoxybenzoyl chloride (**7a**) (483 mg, 2.43 mmol) to yield **15** (428 mg, 62%). Purification was carried out on a silica gel column using hexanes/ethyl acetate (3:1) to provide the pure compound as colorless solid, mp 59–62 °C. $^1\text{H NMR}$ (CDCl_3 , 400 MHz) δ 8.56 (s, 1H), 8.19 (d, J = 8.2 Hz, 1H), 7.90 (d, J = 8.8 Hz, 2H), 7.66 (dd, J = 8.0 Hz, 2H), 6.96 (d, J = 8.8 Hz, 1H), 6.93 (d, J = 7.5 Hz, 1H), 3.98 (t, J = 6.5 Hz, 2H), 2.72 (q, J = 7.6 Hz, 2H), 1.85 (m, 2H), 1.28 (t, J = 7.6 Hz, 3H), 1.06 (t, J = 7.4 Hz, 3H); $^{13}\text{C NMR}$ (CDCl_3 , 100 MHz) δ 165.6, 162.7, 162.5, 151.5, 139.1, 129.5, 126.7, 118.2, 114.8, 111.5, 70.1, 31.4, 23.1, 14.2, 10.9; ESI-MS m/z 285.13 (M+H, 100); Anal. Calcd for $\text{C}_{17}\text{H}_{20}\text{N}_2\text{O}_2$ (284.12): C, 71.81; H, 7.09; N, 9.85. Found: C, 71.62; H, 7.40; N, 9.92.

6.6.3.9. Allyl 4-(allyloxy)benzoate (17) and 4-(Allyloxy)benzoic acid (18). Allyl bromide (2.5 g, 20.7 mmol) was added to 4-hydroxybenzoic acid (**16**) (700 mg, 5.07 mmol) and NaOH (452 mg, 11.3 mmol) in 20 mL 1:1 H_2O /ethanol (v/v). The solution was heated to reflux overnight, and then solvent was removed under reduced pressure to yield the crude products. Purification was carried out on a silica gel column using hexanes/ethyl acetate (3:1) to provide the pure compounds **17** (570 mg) and **18** (305 mg) as colorless solids. Compound **17** (834 mg, 3.82 mmol) and NaOH (153 mg, 3.83 mmol) were dissolved in 10 mL 1:1 H_2O /ethanol (v/v) and the solution was heated to reflux overnight. The solvent was removed under reduced pressure and the solid was dissolved in H_2O and acidified. The aqueous solution was extracted with ethyl acetate (3 \times 30 mL), and then the organic layer was combined and dried with anhydrous Na_2SO_4 . Compound **18** was obtained and further purified by recrystallization in 1:1 hexanes/ethyl acetate (650 mg, 95%). Compound **17**: $^1\text{H NMR}$ (CDCl_3 , 300 MHz) δ 8.02 (d, J = 8.1 Hz, 2H), 6.91 (d, J = 8.1 Hz, 2H), 6.01

(m, 2H), 5.40 (d, J = 17.1 Hz, 2H), 5.28 (m, 2H), 4.80 (d, J = 5.7 Hz, 2H), 4.53 (d, J = 4.8 Hz, 2H). Compound **18**: $^1\text{H NMR}$ (CDCl_3 , 300 MHz) δ 8.08 (d, J = 8.8 Hz, 2H), 6.98 (d, J = 8.8 Hz, 2H), 6.08 (m, 1H), 5.45 (d, J = 17.1 Hz, 1H), 5.35 (d, J = 10.5 Hz, 1H), 4.64 (d, J = 5.1 Hz, 2H).

6.6.3.10. 4-Propoxy-*N*-(6-(propylamino)pyridin-2-yl)benzamide (19). Compound **12** (212 mg, 0.63 mmol), propylamine (50 mg, 0.85 mmol), $\text{Pd}_2(\text{dba})_3$ (42 mg, 0.045 mmol), 2,2'-bis(diphenylphosphino)-1,1'-binaphthyl (*rac*-BINAP, 62 mg, 0.10 mmol), NaO-*t*-Bu (320 mg, 3.29 mmol), and toluene (6 mL) were added to an oven-dried reaction vessel that was purged with argon for approximately 5 min. The reaction mixture was then heated to 70 °C under argon until compound **12** was consumed as determined by TLC. The reaction mixture was then allowed to cool to room temperature and ethyl acetate (10 mL) was added. The solid was removed by filtration and the filtrate was concentrated under reduced pressure to give the crude product. Purification was carried out on a silica gel column using hexanes/ethyl acetate (3:1) to provide the pure compound (152 mg, 77%) as an off-white oil. $^1\text{H NMR}$ (CDCl_3 , 300 MHz) δ 8.36 (s, 1H), 7.85 (d, J = 8.7 Hz, 2H), 7.62 (d, J = 7.8 Hz, 1H), 7.46 (dd, J = 7.8 Hz, 1H), 6.93 (d, J = 8.7 Hz, 2H), 6.16 (d, J = 8.1 Hz, 1H), 4.49 (t, J = 4.8 Hz, 1H), 3.96 (t, J = 6.6 Hz, 2H), 3.18 (q, J = 6.3 Hz, 2H), 1.83 (m, 2H), 1.60 (m, 2H), 1.05 (t, J = 7.2 Hz, 3H), 0.97 (t, J = 7.2 Hz, 3H); $^{13}\text{C NMR}$ (CDCl_3 , 75 MHz) δ 165.0, 162.2, 157.8, 150.2, 139.7, 129.0, 126.6, 114.4, 102.2, 102.1, 69.7, 44.0, 22.8, 22.5, 11.6, 10.5; ESI-MS m/z 314.14 (M + H, 100); Anal. Calcd for $\text{C}_{18}\text{H}_{23}\text{N}_3\text{O}_2$ (313.18): C, 68.98; H, 7.40; N, 13.41. Found: C, 69.28; H, 7.79; N, 13.02.

6.6.3.11. 4-Propoxy-*N*-(6-(butylamino)pyridin-2-yl)benzamide (20). The reaction was similar to the one used to prepare compound **19** with compound **12** (204 mg, 0.61 mmol), butylamine (63 mg, 0.86 mmol), $\text{Pd}_2(\text{dba})_3$ (47 mg, 0.068 mmol), 2,2'-bis(diphenylphosphino)-1,1'-binaphthyl (*rac*-BINAP, 68 mg, 0.11 mmol), NaO-*t*-Bu (321 mg, 3.29 mmol), and toluene (6 mL) to yield **20** (155 mg, 78%). Purification was carried out on a silica gel column using hexanes/ethyl acetate (3:1) to provide the pure compound as an off-white oil. $^1\text{H NMR}$ (CDCl_3 , 300 MHz) δ 8.19 (s, 1H), 7.87 (d, J = 8.4 Hz, 2H), 7.62 (d, J = 8.1 Hz, 1H), 7.50 (dd, J = 8.1 Hz, 1H), 6.97 (d, J = 8.7 Hz, 2H), 6.17 (d, J = 8.1 Hz, 1H), 4.37 (br, 1H), 3.99 (t, J = 6.3 Hz, 2H), 3.25 (q, J = 6.3 Hz, 2H), 1.85 (m, 2H), 1.61 (m, 2H), 1.44 (m, 2H), 1.07 (t, J = 7.5 Hz, 3H), 0.98 (t, J = 7.2 Hz, 3H); $^{13}\text{C NMR}$ (CDCl_3 , 75 MHz) δ 165.0, 162.2, 157.8, 150.2, 139.8, 129.0, 126.6, 114.4, 102.1, 102.0, 69.7, 41.9, 31.7, 22.5, 20.2, 13.9, 10.5; ESI-MS m/z 328.16 (M+H, 100); Anal. Calcd for $\text{C}_{19}\text{H}_{25}\text{N}_3\text{O}_2$ (327.19): C, 69.70; H, 7.70; N, 12.83. Found: C, 70.32; H, 7.72; N, 12.56.

6.6.3.12. *N*-(6-(Pentylamino)pyridin-2-yl)-4-propoxybenzamide (21). The reaction was similar to the one used to prepare compound **19** with compound **12** (203 mg, 0.61 mmol), amylamine (63 mg, 0.72 mmol), $\text{Pd}_2(\text{dba})_3$ (46 mg, 0.049 mmol), 2,2'-bis(diphenylphosphino)-1,1'-binaphthyl (*rac*-BINAP, 65 mg, 0.10 mmol), NaO-*t*-Bu (325 mg, 3.3 mmol), and toluene (5 mL) to yield **21** (145 mg, 70%). Purification was carried out on a silica gel column using hexanes/ethyl acetate (3:1) to provide the pure compound as an off-white oil. $^1\text{H NMR}$ (CDCl_3 , 300 MHz) δ 8.22 (s, 1H), 7.87 (d, J = 8.1 Hz, 2H), 7.62 (d, J = 7.8 Hz, 1H), 7.50 (dd, J = 8.1 Hz, 1H), 6.96 (d, J = 8.1 Hz, 2H), 6.17 (d, J = 8.1 Hz, 1H), 4.39 (br, 1H), 3.99 (t, J = 6.3 Hz, 2H), 3.24 (m, 2H), 1.85 (m, 2H), 1.62 (m, 2H), 1.38 (m, 4H), 1.07 (t, J = 7.2 Hz, 3H), 0.93 (m, 3H); $^{13}\text{C NMR}$ (CDCl_3 , 75 MHz) δ 165.0, 162.2, 157.8, 150.2, 139.8, 129.0, 126.6, 114.4, 102.1, 102.0, 69.7, 42.2, 29.3, 29.2, 22.5, 14.0, 10.5; ESI-MS m/z 342.16 (M + H, 100).

6.6.3.13. N-(6-(Hexylamino)pyridin-2-yl)-4-propoxybenzamide (22).

The reaction was similar to the one used to prepare compound **19** with compound **12** (204 mg, 0.61 mmol), hexylamine (77 mg, 0.76 mmol), Pd₂(dba)₃ (43 mg, 0.045 mmol), 2,2'-bis(diphenylphosphino)-1,1'-binaphthyl (*rac*-BINAP, 61 mg, 0.10 mmol), NaO-*t*-Bu (325 mg, 3.3 mmol), and toluene (5 mL) to yield **22** (138 mg, 64%). Purification was carried out on a silica gel column using hexanes/ethyl acetate (3:1) to provide the pure compound as an off-white oil. ¹H NMR (CDCl₃, 300 MHz) δ 8.26 (s, 1H), 7.86 (d, *J* = 8.7 Hz, 2H), 7.62 (d, *J* = 7.8 Hz, 1H), 7.49 (dd, *J* = 8.1 Hz, 1H), 6.95 (d, *J* = 8.7 Hz, 2H), 6.16 (d, *J* = 8.1 Hz, 1H), 4.41 (br, 1H), 3.98 (t, *J* = 6.3 Hz, 2H), 3.22 (m, 2H), 1.85 (m, 2H), 1.59 (m, 2H), 1.35 (m, 6H), 1.06 (t, *J* = 7.2 Hz, 3H), 0.91 (t, *J* = 6.9 Hz, 3H); ¹³C NMR (CDCl₃, 75 MHz) δ 165.0, 162.2, 157.8, 150.2, 139.8, 129.0, 126.6, 114.4, 102.1, 102.0, 69.7, 42.2, 31.6, 29.6, 26.7, 22.6, 22.5, 14.0, 10.5; ESI-MS *m/z* 356.18 (M+H, 100).

6.6.3.14. N-(6-(Phenylamino)pyridin-2-yl)-4-propoxybenzamide (23).

The reaction was similar to the one used to prepare compound **19** with compound **12** (112 mg, 0.33 mmol), aniline (100 mg, 1.08 mmol), Pd₂(dba)₃ (26 mg, 0.028 mmol), 2,2'-bis(diphenylphosphino)-1,1'-binaphthyl (*rac*-BINAP, 34 mg, 0.055 mmol), NaO-*t*-Bu (192 mg, 2.0 mmol), and toluene (6 mL) to yield **23** (115 mg, 99%). Purification was carried out on a silica gel column using hexanes/ethyl acetate (3:1) to provide the pure compound as a colorless solid, mp 112–115 °C. ¹H NMR (CDCl₃, 300 MHz) δ 8.49 (s, 1H), 7.83 (m, 3H), 7.55 (dd, *J* = 8.1 Hz, 1H), 7.32 (m, 4H), 7.05 (m, 1H), 6.93 (d, *J* = 8.7 Hz, 2H), 6.76 (s, 1H), 6.63 (d, *J* = 8.1 Hz, 1H), 3.97 (t, *J* = 6.6 Hz, 2H), 1.85 (m, 2H), 1.07 (t, *J* = 7.5 Hz, 3H); ¹³C NMR (CDCl₃, 75 MHz) δ 165.3, 162.3, 154.7, 150.4, 140.3, 140.1, 129.2, 129.1, 126.4, 122.8, 120.4, 114.4, 104.7, 104.3, 69.7, 22.5, 10.5; ESI-MS *m/z* 348.13 (M+H, 100).

6.6.3.15. N-(6-((2-Fluorophenyl)amino)pyridin-2-yl)-4-propoxybenzamide (24).

The reaction was similar to the one used to prepare compound **19** with compound **12** (120 mg, 0.36 mmol), 2-fluoroaniline (80 mg, 0.72 mmol), Pd₂(dba)₃ (25 mg, 0.027 mmol), 2,2'-bis(diphenylphosphino)-1,1'-binaphthyl (*rac*-BINAP, 37 mg, 0.06 mmol), NaO-*t*-Bu (190 mg, 1.95 mmol), and toluene (6 mL) to yield **24** (97 mg, 74%). Purification was carried out on a silica gel column using hexanes/ethyl acetate (3:1) to provide the pure compound as a colorless solid, mp 87–90 °C. ¹H NMR (CDCl₃, 300 MHz) δ 8.29 (s, 1H), 7.98 (dd, *J* = 8.1 Hz, 1H), 7.88 (dd, *J* = 8.1 Hz, 3H), 7.61 (dd, *J* = 8.1 Hz, 1H), 7.14 (m, 2H), 7.01 (m, 3H), 6.60 (d, 1H), 6.50 (s, 1H), 4.01 (t, *J* = 6.3 Hz, 2H), 1.85 (m, 2H), 1.08 (t, *J* = 7.5 Hz, 3H); ¹³C NMR (CDCl₃, 75 MHz) δ 165.1, 162.4, 153.8, 150.2, 140.1, 129.1, 126.4, 124.3, 124.2, 122.5, 122.4, 120.9, 115.5, 115.2, 114.5, 105.2, 69.8, 22.5, 10.5; ESI-MS *m/z* 366.12 (M+H, 100).

6.6.3.16. N-(6-((3-Fluorophenyl)amino)pyridin-2-yl)-4-propoxybenzamide (25).

The reaction was similar to the one used to prepare compound **19** with compound **12** (150 mg, 0.45 mmol), 3-fluoroaniline (90 mg, 0.81 mmol), Pd₂(dba)₃ (30 mg, 0.032 mmol), 2,2'-bis(diphenylphosphino)-1,1'-binaphthyl (*rac*-BINAP, 39 mg, 0.063 mmol), NaO-*t*-Bu (190 mg, 1.95 mmol), and toluene (5 mL) to yield **25** (147 mg, 90%). Purification was carried out on a silica gel column using hexanes/ethyl acetate (3:1) to provide the pure compound as a colorless solid, mp 108–110 °C. ¹H NMR (CDCl₃, 300 MHz) δ 8.24 (s, 1H), 7.88 (m, 3H), 7.62 (dd, *J* = 8.1 Hz, 1H), 7.28 (m, 2H), 7.02 (m, 3H), 6.74 (m, 1H), 6.62 (d, *J* = 8.1 Hz, 1H), 6.44 (br, 1H), 4.02 (t, *J* = 6.6 Hz, 2H), 1.87 (m, 2H), 1.08 (t, *J* = 7.5 Hz, 3H); ¹³C NMR (CDCl₃, 75 MHz) δ 165.1, 162.4, 161.8, 153.7, 150.3, 142.0, 140.2, 130.3, 129.1, 126.3, 114.8, 114.5, 109.1, 106.6, 106.3, 105.3, 69.8, 22.5, 10.5; ESI-MS *m/z* 366.09 (M + H, 100); Anal. Calcd for C₂₁H₂₀FN₃O₂ (365.40): C, 69.03; H, 5.52; N, 11.50. Found: C, 68.92; H, 5.48; N, 11.51.

6.6.3.17. N-(6-((4-Fluorophenyl)amino)pyridin-2-yl)-4-propoxybenzamide (26).

The reaction was similar to the one used to prepare **19** with compound **12** (114 mg, 0.34 mmol), 4-fluoroaniline (60 mg, 0.54 mol), Pd₂(dba)₃ (24 mg, 0.026 mmol), 2,2'-bis(diphenylphosphino)-1,1'-binaphthyl (*rac*-BINAP, 34 mg, 0.055 mmol), NaO-*t*-Bu (186 mg, 1.91 mmol), and toluene (5 mL) to yield **26** (86 mg, 69%). Purification was carried out on a silica gel column using hexanes/ethyl acetate (3:1) to provide the pure compound as a colorless solid, mp 135–138 °C. ¹H NMR (CDCl₃, 300 MHz) δ 8.21 (s, 1H), 7.82 (d, 2H), 7.78 (d, 1H), 7.55 (m, 1H), 7.28 (m, 2H), 7.05 (m, 4H), 6.52 (d, 1H), 6.25 (s, 1H), 4.02 (m, 2H), 1.86 (m, 2H), 1.11 (m, 3H); ¹³C NMR (CDCl₃, 75 MHz) δ 165.1, 162.4, 154.9, 150.2, 140.2, 129.1, 126.3, 123.0, 122.9, 116.1, 115.8, 114.5, 104.5, 103.9, 69.8, 22.5, 10.5; ESI-MS *m/z* 366.07 (M+H, 100).

6.6.3.18. N-(6-((4-Chlorophenyl)amino)pyridin-2-yl)-4-propoxybenzamide (27).

The reaction was similar to the one used to prepare **19** with compound **12** (115 mg, 0.34 mmol), 4-chloroaniline (61 mg, 0.48 mol), Pd₂(dba)₃ (25 mg, 0.027 mmol), 2,2'-bis(diphenylphosphino)-1,1'-binaphthyl (*rac*-BINAP, 35 mg, 0.056 mmol), NaO-*t*-Bu (187 mg, 1.92 mmol), and toluene (5 mL) to yield **27** (76 mg, 58%). Purification was carried out on a silica gel column using hexanes/ethyl acetate (3:1) to provide the pure compound as a colorless solid, mp 143–146 °C. ¹H NMR (CDCl₃, 300 MHz) δ 8.30 (s, 1H), 7.84 (m, 3H), 7.58 (dd, *J* = 7.8 Hz, 1H), 7.29 (m, 4H), 6.97 (d, *J* = 9.0 Hz, 2H), 6.55 (d, *J* = 8.1 Hz, 1H), 6.50 (s, 1H), 4.00 (t, *J* = 6.6 Hz, 2H), 1.86 (m, 2H), 1.08 (t, *J* = 7.5 Hz, 3H); ¹³C NMR (CDCl₃, 75 MHz) δ 165.1, 162.4, 154.1, 150.3, 140.2, 138.9, 129.2, 129.1, 127.5, 126.3, 121.3, 114.5, 105.0, 104.6, 69.8, 22.5, 10.5; ESI-MS *m/z* 382.09 (M + H, 100); Anal. Calcd for C₂₁H₂₀ClN₃O₂ (381.86): C, 66.05; H, 5.28; N, 11.00. Found: C, 66.09; H, 5.24; N, 11.07.

6.6.3.19. N-(6-((4-Methoxyphenyl)amino)pyridin-2-yl)-4-propoxybenzamide (28).

The reaction was similar to the one used to prepare **19** with compound **12** (118 mg, 0.35 mmol), 4-methoxyaniline (72 mg, 0.59 mol), Pd₂(dba)₃ (27 mg, 0.029 mmol), 2,2'-bis(diphenylphosphino)-1,1'-binaphthyl (*rac*-BINAP, 35 mg, 0.056 mmol), NaO-*t*-Bu (180 mg, 1.85 mmol), and toluene (6 mL) to yield **28** (107 mg, 80%). Purification was carried out on a silica gel column using hexanes/ethyl acetate (3:1) to provide the pure compound as a colorless solid, mp 103–105 °C. ¹H NMR (CDCl₃, 300 MHz) δ 8.26 (s, 1H), 7.87 (d, *J* = 9.0 Hz, 2H), 7.75 (d, *J* = 7.8 Hz, 1H), 7.53 (dd, *J* = 8.1 Hz, 1H), 7.25 (d, *J* = 8.7 Hz, 2H), 6.98 (d, *J* = 8.7 Hz, 2H), 6.92 (d, *J* = 9.0 Hz, 2H), 6.44 (d, *J* = 8.4 Hz, 1H), 6.26 (s, 1H), 4.01 (t, *J* = 6.6 Hz, 2H), 3.84 (s, 3H), 1.85 (m, 2H), 1.08 (t, *J* = 7.5 Hz, 3H); ¹³C NMR (CDCl₃, 75 MHz) δ 165.1, 162.3, 156.3, 155.9, 150.3, 140.1, 133.0, 129.1, 126.4, 124.1, 114.6, 114.4, 103.9, 103.2, 69.7, 55.5, 22.5, 10.5; ESI-MS *m/z* 378.15 (M+H, 81), 400.13 (M+Na, 100).

6.6.3.20. N-(6-(Benzylamino)pyridin-2-yl)-4-propoxybenzamide (29).

The reaction was similar to the one used to prepare **19** with compound **12** (113 mg, 0.34 mmol), benzylamine (70 mg, 0.65 mol), Pd₂(dba)₃ (24 mg, 0.026 mmol), 2,2'-bis(diphenylphosphino)-1,1'-binaphthyl (*rac*-BINAP, 38 mg, 0.06 mmol), NaO-*t*-Bu (190 mg, 1.95 mmol), and toluene (5 mL) to yield **29** (83 mg, 68%). Purification was carried out on a silica gel column using hexanes/ethyl acetate (3:1) to provide the pure compound as a colorless solid, mp 87–89 °C. ¹H NMR (CDCl₃, 300 MHz) δ 8.33 (s, 1H), 7.86 (d, *J* = 8.7 Hz, 2H), 7.68 (d, *J* = 7.8 Hz, 1H), 7.48 (dd, *J* = 8.1 Hz, 1H), 7.35 (m, 4H), 7.30 (m, 1H), 6.95 (d, *J* = 9.0 Hz, 2H), 6.19 (d, *J* = 8.1 Hz, 1H), 4.87 (br, 1H), 4.50 (d, *J* = 6.0 Hz, 2H), 3.98 (t, *J* = 6.6 Hz, 2H), 1.85 (m, 2H), 1.08 (t, *J* = 7.5 Hz, 3H); ¹³C NMR (CDCl₃, 75 MHz) δ 165.0, 162.2, 157.5, 150.2, 139.8, 139.3, 129.0,

128.7, 127.4, 127.3, 126.5, 114.4, 102.7, 102.6, 69.7, 46.1, 22.5, 10.5; ESI-MS m/z 362.13 (M+H, 100).

6.6.3.21. N-(6-(Piperidin-1-yl)pyridin-2-yl)-4-propoxybenzamide (30).

The reaction was similar to the one used to prepare **19** with compound **12** (161 mg, 0.48 mmol), piperidine (75 mg, 0.88 mol), Pd₂(dba)₃ (24 mg, 0.026 mmol), 2,2'-bis(diphenylphosphino)-1,1'-binaphthyl (*rac*-BINAP, 42 mg, 0.07 mmol), NaO-*t*-Bu (196 mg, 2.01 mmol), and toluene (5 mL) to yield **30** (106 mg, 65%). Purification was carried out on a silica gel column using hexanes/ethyl acetate (3:1) to provide the pure compound as a colorless solid, mp 89–92 °C. ¹H NMR (CDCl₃, 300 MHz) δ 8.19 (s, 1H), 7.88 (d, $J = 8.7$ Hz, 2H), 7.61 (d, $J = 7.5$ Hz, 1H), 7.53 (dd, $J = 7.8$ Hz, 1H), 6.98 (d, $J = 8.4$ Hz, 2H), 6.42 (d, $J = 8.1$ Hz, 1H), 4.00 (t, $J = 6.6$ Hz, 2H), 3.52 (m, 4H), 1.86 (m, 2H), 1.66 (m, 6H), 1.08 (t, $J = 7.5$ Hz, 3H); ¹³C NMR (CDCl₃, 75 MHz) δ 165.0, 162.1, 158.4, 150.0, 139.7, 129.0, 126.7, 114.4, 102.7, 101.9, 69.7, 46.2, 25.5, 24.7, 22.5, 10.5; ESI-MS m/z 340.10 (M+H, 100); Anal. Calcd for C₂₀H₂₅N₃O₂ (339.43): C, 70.77; H, 7.42; N, 12.38. Found: C, 70.75; H, 7.37; N, 12.14.

6.6.3.22. N-(6-bromopyridin-2-yl)acetamide (31).

2-Amino-6-bromopyridine (**6b**) (730 mg, 4.22 mmol) and triethylamine (588 μL, 4.22 mmol) in 5 mL DCM was added to acetyl chloride (2 mL, 28 mmol) in DCM (5 mL). The solution was stirred overnight, then was washed with saturated NaHCO₃, H₂O, brine and dried with anhydrous Na₂SO₄. The crude product was obtained by removing the solvent under reduced pressure and further purified by recrystallization in ethyl acetate (860 mg, 95%). ¹H NMR (CDCl₃, 300 MHz) δ 8.17 (d, $J = 8.1$ Hz, 1H), 7.98 (br, 1H), 7.57 (dd, $J = 7.8$ Hz, 1H), 7.23 (d, $J = 7.5$ Hz, 1H), 2.22 (s, 3H).

6.6.3.23. N-(6-(propylamino)pyridin-2-yl)acetamide (32).

The reaction was similar to the one used to prepare **19** with compound **31** (455 mg, 2.12 mmol), propylamine (144 mg, 2.44 mmol), Pd₂(dba)₃ (129 mg, 0.14 mmol), 2,2'-bis(diphenylphosphino)-1,1'-binaphthyl (*rac*-BINAP, 195 mg, 0.31 mmol), NaO-*t*-Bu (1.07 g, 10.5 mmol), and toluene (5 mL) to yield **32** (215 mg, 53%). Purification was carried out on a silica gel column using hexanes/ethyl acetate (3:1) to provide the pure compound as a colorless solid. ¹H NMR (CDCl₃, 300 MHz) δ 8.23 (s, 1H), 7.43 (m, 2H), 6.13 (m, 1H), 4.48 (bs, 1H), 3.17 (m, 2H), 2.10 (s, 3H), 1.59 (m, 2H), 0.96 (t, $J = 7.2$ Hz, 3H).

6.6.3.24. N-(6-(butylamino)pyridin-2-yl)acetamide (33).

The reaction was similar to the one used to prepare **19** with compound **31** (400 mg, 1.86 mmol), butylamine (148 mg, 2.03 mmol), Pd₂(dba)₃ (127 mg, 0.14 mmol), 2,2'-bis(diphenylphosphino)-1,1'-binaphthyl (*rac*-BINAP, 179 mg, 0.28 mmol), NaO-*t*-Bu (1.0 g, 10.5 mmol), and toluene (5 mL) to yield **33** (207 mg, 54%). Purification was carried out on a silica gel column using hexanes/ethyl acetate (3:1) to provide the pure compound as a colorless solid. ¹H NMR (CDCl₃, 300 MHz) δ 8.05 (s, 1H), 7.43 (m, 2H), 6.13 (m, 1H), 4.41 (bs, 1H), 3.21 (m, 2H), 2.12 (s, 3H), 1.59 (m, 2H), 1.39 (m, 2H), 0.94 (t, $J = 7.5$ Hz, 3H).

6.6.3.25. 4-(Allyloxy)-N-(6-(propylamino)pyridin-2-yl)benzamide (34).

Compound **32** (165 mg, 0.85 mmol) and NaOH (90 mg, 2.25 mmol) were heated to reflux in 5 mL 1:1 H₂O/ethanol (v:v) by the procedure used to hydrolyze ester **17** to yield pure *N*²-propylpyridine-2,6-diamine. *N*²-propylpyridine-2,6-diamine (85 mg, 0.56 mmol) and 4-allyloxybenzoyl chloride (**7b**, 77 mg, 0.39 mmol) were coupled using the procedure employed to prepare **8** to provide **34** (63 mg, 52%). Purification was carried out on a silica gel column using hexanes/ethyl acetate (3:1) to afford the pure compound as an off-white oil. It was further converted into its hydrochloric acid salt, mp 175–177 °C. ¹H NMR (CDCl₃, 300 MHz) δ 15.08 (s, 1H), 11.34 (s, 1H), 8.24 (d, $J = 8.7$ Hz, 2H),

7.77 (d, $J = 8.1$ Hz, 1H), 7.68 (dd, $J = 8.4$ Hz, 1H), 7.22 (br, 1H), 6.99 (d, $J = 8.7$ Hz, 2H), 6.54 (d, $J = 8.4$ Hz, 1H), 6.04 (m, 1H), 5.43 (d, 1H), 5.22 (d, $J = 9.6$ Hz, 1H), 4.59 (d, $J = 5.4$ Hz, 2H), 3.36 (m, 2H), 1.75 (m, 2H), 1.04 (t, $J = 7.2$ Hz, 3H); ¹³C NMR (CDCl₃, 300 MHz) δ 166.0, 162.7, 151.3, 145.1, 132.4, 130.6, 124.2, 118.3, 114.8, 101.0, 68.9, 44.6, 22.0, 11.3; MS m/z 312.11 (M+H, 100); Anal. Calcd for C₁₈H₂₂ClN₃O₂ (347.56): C, 62.15; H, 6.37; N, 12.08. Found: C, 61.89; H, 6.34; N, 11.87.

6.6.3.26. 4-(Allyloxy)-N-(6-(butylamino)pyridin-2-yl)benzamide (35).

Compound **33** (208 mg, 1.0 mmol) and NaOH (180 mg, 4.5 mmol) were heated to reflux in 10 mL 1:1 H₂O/ethanol (v:v) by the procedure used to hydrolyze ester **17** to yield pure *N*²-butylpyridine-2,6-diamine. *N*²-butylpyridine-2,6-diamine (166 mg, 1 mmol) and 4-allyloxybenzoyl chloride (**7b**, 197.4 mg, 1 mmol) were coupled using the procedure employed to prepare **8** to yield **35** (258 mg, 79%). Purification was carried out on a silica gel column using hexanes/ethyl acetate (3:1) to afford the pure compound as an off-white oil. It was further converted into its hydrochloric acid salt, mp 160–164 °C. ¹H NMR (CDCl₃, 300 MHz) δ 15.36 (s, 1H), 11.16 (s, 1H), 8.23 (d, $J = 8.7$ Hz, 2H), 7.84 (d, $J = 8.1$ Hz, 1H), 7.74 (dd, $J = 8.4$ Hz, 1H), 7.01 (d, $J = 8.7$ Hz, 2H), 6.66 (br, 1H), 6.46 (d, $J = 8.4$ Hz, 1H), 6.06 (m, 1H), 5.44 (d, $J = 17.4$ Hz, 1H), 5.33 (d, $J = 10.5$ Hz, 1H), 4.61 (d, $J = 5.1$ Hz, 2H), 3.39 (m, 2H), 1.71 (m, 2H), 1.47 (m, 2H), 0.98 (t, $J = 7.5$ Hz, 3H); ¹³C NMR (CDCl₃, 75 MHz) δ 165.6, 162.7, 151.3, 145.4, 145.2, 132.4, 130.5, 126.7, 124.2, 118.3, 114.9, 101.2, 68.9, 42.8, 30.7, 20.0, 13.9; ESI-MS m/z 326.11 (M+H, 100); Anal. Calcd for C₁₉H₂₄ClN₃O₂ (361.16): C, 63.06; H, 6.68; N, 11.61. Found: C, 63.11; H, 6.53; N, 11.45.

Author contributions

Experimental design: Bitna Yi, Tatiana González-Cestari, Brandon J. Henderson, Ryan E. Pavlovicz, Karl Werbovetz, Chenglong Li.

Pharmacological assays: Bitna Yi, Tatiana González-Cestari, Brandon J. Henderson.

Data analyses and interpretation: Bitna Yi, Tatiana González-Cestari, Sihui Long, Karl Werbovetz, Dennis McKay.

Pharmacophore design: Brandon Henderson.

Ligand-based virtual screening: Brandon Henderson

Synthetic chemistry: Sihui Long

Manuscript writing: Bitna Yi, Sihui Long, Karl Werbovetz, Dennis McKay.

Acknowledgements

This work was supported by the National Institutes of Health National Institute on Drug Abuse (Grant DA029433). All stably transfected human cell lines were kindly provided by Dr. Jon M. Lindstrom, Department of Neuroscience School of Medicine, University of Pennsylvania, Philadelphia, PA.

References and notes

- Dani, J. A.; Bertrand, D. *Annu. Rev. Pharmacol. Toxicol.* **2007**, *47*, 699.
- Lloyd, G. K.; Menzaghi, F.; Bontempi, B.; Suto, C.; Siegel, R.; Akong, M.; Stauderman, K.; Velicelebi, G.; Johnson, E.; Harpold, M. M.; Rao, T. S.; Sacca, A. I.; Chavez-Noriega, L. E.; Washburn, M. S.; Vernier, J. M.; Cosford, N. D. P.; McDonald, L. A. *Life Sci.* **1998**, *62*, 1601.
- Taly, A.; Corringier, P.-J.; Guedin, D.; Lestage, P.; Changeux, J.-P. *Nat. Rev. Drug Disc.* **2009**, *8*, 733.
- Lukas, R. J.; Changeux, J.-P.; le Novère, N.; Albuquerque, E. X.; Balfour, J. K.; Berg, D. K.; Bertrand, D.; Chiappinelli, V. A.; Clarke, P. B. S.; Collins, A. C.; Dani, J. A.; Grady, S. R.; Kellar, K. J.; Lindstrom, J. M.; Marks, M. J.; Quik, M.; Taylor, P. W.; Wonnacott, S. *Pharmacol. Rev.* **1999**, *51*, 397.
- Papke, R. L. *Prog. Neurobiol.* **1993**, *41*, 509.
- Gotti, C.; Zoli, M.; Clementi, F. *Trends Pharmacol. Sci.* **2006**, *27*, 482.
- Goldman, D.; Deneris, E.; Luyten, W.; Kochhar, A.; Patrick, J.; Heinemann, S. *Cell* **1987**, *48*, 965.

8. Cassels, B. K.; Bermudez, I.; Dajas, F.; Abin-Carriquiry, A.; Wonnacott, S. *Drug Discovery Today* **2007**, *10*, 1657.
9. Tapper, A. R.; McKinney, S. L.; Nashmi, R.; Schwarz, J.; Deshpande, P.; Labarca, C.; Whiteaker, P.; Marks, M. J.; Collins, A. C.; Lester, H. A. *Science* **2004**, *306*, 1029.
10. Tapper, A. R.; McKinney, S. L.; Marks, M. J.; Lester, H. A. *Physiol. Genomics* **2007**, *31*, 422.
11. Picciotto, M. R.; Zoli, M.; Rimondini, R.; Léna, C.; Marubio, L. M.; Pich, E. M.; Fuxe, K.; Changeux, J.-P. *Nature* **1998**, *391*, 173.
12. Picciotto, M. R.; Zoli, M.; Zachariou, V.; Changeux, J.-P. *Biochem. Soc. Trans.* **1997**, *25*, 824.
13. Henderson, B. J.; Carper, D. J.; González-Cestari, T. F.; Yi, B.; Mahasenan, K. V.; Pavlovicz, R. E.; Dalefield, M. L.; Coleman, R. S.; Li, C.; McKay, D. B. *J. Med. Chem.* **2011**, *54*, 8681.
14. Mahasenan, K. V.; Pavlovicz, R. E.; Henderson, B. J.; González-Cestari, T. F.; Yi, B.; McKay, D. B.; Li, C. *ACS. Med. Chem. Lett.* **2011**. <http://dx.doi.org/10.1021/ml2001714>.
15. González-Cestari, T. F.; Henderson, B. J.; Pavlovicz, R. E.; McKay, S. B.; El Hajj, R. A.; Pulipaka, A. B.; Orac, C. M.; Reed, D. D.; Boyd, R. T.; Zhu, M. X.; Li, C.; Bergmeier, S. C.; McKay, D. B. *J. Pharmacol. Exp. Ther.* **2009**, *328*, 504.
16. Henderson, B. J.; Pavlovicz, R. E.; Allen, J. D.; Gonzalez-Cestari, T. F.; Orac, C. M.; Bonnel, A. B.; Zhu, M. X.; Boyd, R. T.; Li, C.; Bergmeier, S. C.; McKay, D. B. *J. Pharmacol. Exp. Ther.* **2010**, *334*, 761.
17. Henderson, B. J.; González-Cestari, T. F.; Yi, B.; Pavlovicz, R. E.; Boyd, R. T.; Li, C.; Bergmeier, S. C.; McKay, D. B. *ACS Chem. Neurosci.* **2012**. <http://dx.doi.org/10.1021/cn300035f>.
18. Pavlovicz, R. E.; Henderson, B. J.; Bonnel, A. B.; Boyd, R. T.; McKay, D. B.; Li, C. *PLoS ONE* **2011**. <http://dx.doi.org/10.1371/journal.pone.0024949>.
19. Pickaert, G.; Cesario, M.; Ziessel, R. *J. Org. Chem.* **2004**, *69*, 5335.
20. Wagaw, S.; Buchwald, S. L. *J. Org. Chem.* **1996**, *61*, 7240.
21. Jorgensen, W. L. *Science* **2004**, *303*, 1813.
22. Yang, G. F.; Huang, X. *Curr. Pharm. Des.* **2006**, *12*, 4601.
23. Shoichet, B. K.; McGovern, S. L.; Wei, B.; Irwin, J. J. *Curr. Opin. Chem. Biol.* **2002**, *6*, 439–446.
24. Walters, W. P.; Stahl, M.; Murcko, M. A. *Drug Discovery Today* **1998**, *3*, 160.
25. Jain, A. N. *Curr. Opin. Drug Disc. Dev.* **2004**, *7*, 396–403.
26. Floriano, W. B.; Vaidehi, N.; Zamanakos, G.; Goddard, W. A., III. *J. Med. Chem.* **2004**, *47*, 56.
27. McKay, D. B.; Burkman, A. M. *Proc. Soc. Exp. Biol. Med.* **1993**, *203*, 372.
28. McKay, D. B.; Sanchez, A. P. *Pharmacology* **1990**, *40*, 224.
29. Henderson, B. J.; Orac, C. M.; Maciagiewicz, I.; Bergmeier, S. C.; McKay, D. B. *Bioorg. Med. Chem. Lett.* **2012**, *22*, 1797.
30. McKay, D. B.; Cheng, C.; González-Cestari, T. F.; McKay, S. B.; El-Hajj, R.; Bryant, D. L.; Swaan, P. W.; Arason, K. M.; Pulipaka, A. B.; Orac, C. M.; Bergmeier, S. C. *Mol. Pharmacol.* **2007**, *71*, 1288.